SPE
Society of Petroleum Engineers

SPE 22940

A Numerical-Dispersion-Free Method for Modeling the Gas Cycling Process

E.Y. Chang and T.S. Lo, ARCO Oil & Gas Co.
SPE Members

This paper was prepared for presentation at the 66th Annual Technical Conference and Exhibition of the Society of Petroleum Engineers held in Dallas, TX, October 6-9, 1991

ABSTRACT

This paper describes an effective methodology for accurate evaluation of liquid recovery during the gas cycling of condensate reservoirs. First, the fluid flow problem is solved by potential flow, which is shown to be applicable to compressible gas flows also. The mass transfer and phase behavior within the potential flow streamtubes can then be calculated using one dimensional reservoir simulators, which can efficiently control the numerical dispersion errors to any desired level. An example illustrates this method's efficiency and accuracy advantages over conventional finite difference methods.

1. INTRODUCTION

While some reservoirs are exploited for their oil (oil reservoirs), and some for their gas (gas reservoirs), there are reservoirs which can produce substantial amounts of gas and varying quantities of liquids depending on the depletion practice. At discovery, these condensate reservoirs may be filled only with rich gas, which on conditioning in the production separators yields liquid condensate, or they may be filled with gas and small saturations of reservoir liquids which can be easily vaporized and produced as separator liquids or natural gas liquids through similar surface facilities. The amount of separator liquid produced per unit of gas processed, the condensate yield, depends on both the separator configurations and operating conditions.

If these condensate reservoirs are produced for the gas reserves only, the reservoir pressure decline can often lead to retrograde condensation of liquid range hydrocarbon components. This buildup of liquid saturation, especially near the producing well region, may interfere with well productivity, or, at a minimum, leave a valuable resource unexploited. Where economics justifies the injection of either separator or other gases to maintain the reservoir pressure and liquid yield in the produced gas, additional liquid recovery results. The injected gas merely acts as a carrier for transporting the volatile hydrocarbons from the reservoir to the surface.

Evaluations of this process often require more complex and precise tools than those used for other processes because the higher gas compression costs, deferred gas revenues, cost of makeup foreign gases, and higher produced gas oil ratios together render the project economics somewhat less favorable than for typical oil reservoirs. However, where the right set of conditions exist, gas cycling can be effectively used to produce hundreds of millions of liquid barrels[1,2,3].

This paper describes an effective methodology for evaluating this improved liquid recovery process through gas cycling. It is computationally more efficient than the conventional finite difference methods and gives very accurate answers. These results can also be used as benchmarks to validate or estimate the accuracy of other evaluation techniques, such as numerical finite difference models, which are often plagued by numerical dispersion errors.

The method consists of two steps. First, the fluid flow problem is solved, and streamtubes are defined. Then, the saturation and compositional changes along the streamtubes are solved precisely by one-dimensional fully compositional models.

In most instances this decoupling of the fluid flow and phase behavior computations are justified for condensate reservoirs because the gas is the only moving phase, whose mobility is

References and illustrations at end of paper.

insensitive to the slowly changing liquid saturation. The one-dimensional nature of the streamtube model then allows for high precision estimates of gas and liquid recoveries more efficiently than higher dimensional finite difference models of comparable accuracy.

Streamtube models are not new. Popularized by Muskat[4], they have been used for the evaluation of waterfloods and other incompressible flows for decades. What we will show in section 2 is that the potential flow streamlines that are developed for incompressible flows are equally valid for compressible gas flows. The derivation of the streamlines also points out the high level of accuracy afforded by this method, and the few, not very serious, constraints which may limit its applicability.

The example of gas cycling in a condensate reservoir in Section 3 illustrates this method. Conformal mapping is used to generate the exact streamlines, although other methods, such as a conventional finite difference model of the fluid flow problem, will do just as well. The compositional modelling of the stream tubes then provides accurate estimates of the wet gas, dry gas, primary condensate, re-vaporized condensate, and stripped volatile oil recoveries. At reasonable computational loads, these one-dimensional model grids can be refined to control the discretization errors to negligible levels.

The streamtube model results are then compared with finite difference model results in section 4, which also discusses the strengths and limitations of this methodology by way of identifying and assessing the sources of errors in finite difference and streamtube models.

Finally, Section 5 offers some concluding remarks and discusses possible extensions of this method.

2. APPLICABILITY OF POTENTIAL FLOW STREAMLINES IN COMPRESSIBLE GAS FLOWS

To show that streamtubes developed for incompressible potential flows are also valid for compressible gas flows, we will establish in this section the formal equivalence of the mathematical equations for the two types of flows.

The incompressible flows are governed by Laplace's equation for the pressure with the appropriate boundary conditions[4]. The governing equations for compressible flows, in terms of the real gas pseudo-pressure[5], will be shown to have identical structures, and therefore formally the same mathematical solutions. Of course, the physical interpretation of the solutions must take into account the difference between real and pseudo-pressures.

In this discussion, the mathematical equations are expressed in dimensionless forms to better reveal the proper scaling of the various physical parameters.

For most reservoirs, the bed thickness is much smaller than the lateral dimensions along the bedding plane or the distances between wells. Under these conditions, the primary fluid velocities are along the bedding plane, and it is common, and well justified, practice in perturbation analysis to reduce the problem to the two dimensions along the bed for the leading order approximate solutions. The compressible flow is then governed[5] by

$$T \frac{\partial m}{\partial t} = \nabla^2 m \qquad (1)$$

where

$$m = \int_{p_o}^{p} \frac{2p}{\mu Z} \, dp \qquad (2)$$

is the real gas pseudo-pressure[5], and

$$T = \frac{\Phi \mu c L^2}{K} \qquad (3)$$

represents the characteristic transient time scale for the reservoir of characteristic dimension L. Typically, significant changes in well rates of a gas cycling operation result from the infrequent major facility additions, while the transient time scale is at least an order of magnitude smaller. Under these conditions, transients rapidly die out like $\exp(-\alpha t/T)$, and the pseudo-steady-state solution valid most of the time between facility changes is approximated[6] by the leading term in the series solution of eq. (1), i.e., by the solution of:

$$\nabla^2 m = 0 \qquad (4)$$

with a truncation error of the order of $\exp(-10)$. This, of course, is the familiar Laplace equation for the incompressible flow potential.

Likewise, constant pressure or no flow boundary conditions translate directly into similar expressions for the gas pseudo-pressure.

$$m = \text{constant} \qquad (5)$$

or

$$\nabla m \cdot \underline{n} = 0 \qquad (6)$$

on the boundary, or portions thereof.

Thus, the governing equations of the gas pseudo-pressure for the compressible gas flow problem are formally identical with those for the incompressible potential flow problem. The potential flow streamlines are therefore also streamlines for the gas pseudo-pressure.

Moreover, from eq. (2), we see that

$$\nabla m = \frac{2}{\mu Z} \nabla p \qquad (7)$$

which implies that the m-streamlines are everywhere parallel to the pressure gradients, and therefore there is no gas flux across the m-streamlines. This important observation is what permits us to use potential flow streamtubes in our simplified approach to the two-dimensional problem.

It should be noted that due to the non-linear stretching factor $(2/\mu^*Z)$ in eq. (7), the isobaric contours in the gas flow problem are different from those in the potential flow problem.

Another useful result from the potential flow problem is the residence time for each streamtube. For the simple case of a small number of injection sites, the distribution of residence times can be used to estimate the produced gas composition, as shown in Section 3.

Here again, the equations describing the compressible and incompressible flows are formally identical. For example, a one-dimensional incompressible streamtube of length L with end point pressures fixed at P and P+ΔP has a residence time of $(\mu L^2)/(K \Delta P)$. The corresponding residence time for a compressible gas streamtube is $(\langle\mu\rangle L^2)/(K \Delta P)$, with a relative error of the order of $(\Delta P/\langle P\rangle)^2$. For high permeability reservoirs, this relative error is very small, and the potential flow solution can be used directly. For low permeability reservoirs where $(\Delta P/\langle P\rangle)$ may not be negligible, the streamtubes are still valid, but direct integration is required to estimate the residence time.

3. APPLICATION TO A MODEL RESERVOIR PROBLEM

We illustrate the application of this technique to a model problem. Simultaneous with a continuous reservoir pressure decline, dry gas (one with all the condensible liquids removed by separation facilities) is injected into a single injector (or a group of injectors in the same area) into the interior of a reservoir whose areal dimensions are much greater than its thickness, and gas and associated condensate are produced in a row of producers at one end of the reservoir (Figure 2).

The reservoir is initially filled mostly with original gas (wet gas) containing intermediate hydrocarbons recoverable as liquids in separators, and a small immobile saturation of vaporizable liquid, which may be stripped by the injected dry gas. The total liquid recovery associated with the cycling process, therefore, comes from both the reservoir vapor and liquid phases. In this example, they are present in approximately equal amounts. A larger fraction of the first type of liquid is expected to be recovered than the second, because the gas displacement process recovery is more efficient than oil stripping recovery. Note that this problem, although simplified somewhat to facilitate illustration of the new technique, exhibits many complex phenomena associated with the gas cycling process, including the retrograde condensation of liquid from the wet gas under pressure decline and its subsequent re-vaporization by the injection gas.

This problem involves gas cycling in an essentially two-dimensional domain. Since most hydrocarbon reservoirs have a large areal extent in comparison to their thickness, this does not really limit the applicability of the method. In general, an arbitrary number of point injectors and producers may be modelled. Furthermore, a row of producing wells may be approximated by a constant pressure producing boundary, and faults by branch cuts in the complex domain for the potential flow solution. Thus, a fairly complex reservoir may be simulated using this technique, since it may be applied as long as it is possible to obtain a solution for 2-D potential flow within it, whether numerically or analytically.

In general, the solution for 2-D potential flow must be obtained numerically. However, we will demonstrate and validate the method on a simple model problem with one injector in a uniform reservoir which has the shape of a half-ellipse. Since one may vary its aspect ratio, an ellipse can be tailored to fit a wide variety of boundary shapes. In addition, the analytical solution technique for obtaining the potential flow solution is straightforward. The rounded part of the half-ellipse is considered to be impermeable, and the flat axis is made a constant pressure producing boundary.

To begin with, we first obtain a solution for potential flow within a circular boundary with a single injection well and a constant pressure line at its diameter of symmetry (see Figure 1). Employing the method of images in conjunction with the superposition property of linear equations, we find that the complex potential results from a source and a sink inside and outside the circle. For a unit circle with a source on the diameter normal to the constant pressure line and no flow across its boundary, the complex potential is given by[7]

$$\phi + i\psi = q \log \frac{(z-A)(1-Az)}{(z+A)(1+Az)} \qquad (8)$$

where the source strength is $2\pi q$ (area/unit time), A is the source to center distance within the circle, and z is the location in the complex plane. The stream function may be obtained by taking the imaginary part. To obtain the corresponding result for the source being located at an arbitrary position inside the circle, one simply replaces A with A + iB (the new position of the source in the complex plane), yielding

$$\frac{-\psi}{q} = \tan^{-1}\frac{y-B}{A-x} + \tan^{-1}\frac{y+B}{A+x} + \tan^{-1}\frac{Ay+Bx}{1-Ax+By} + \tan^{-1}\frac{Ay+Bx}{1+Ax-By}, \qquad (9)$$

The solution for flow in a circle may be transformed to one valid for another shape by means of conformal mapping in the complex plane. Such a transformation preserves the boundary conditions and the strength of the sources. In addition, the transformed solution based on eq. (2) still satisfies eq. (4) from the previous section (the equation for 2-D potential flow). The transformation required to map the interior of an ellipse to a circle, unfortunately, is expressed in terms of elliptic functions[8].

To avoid this complication, we shall use an approximation. To this end, we employ the rational fraction transformation[9],

$$\zeta = \frac{z}{1 + \varepsilon z^2} \qquad (10)$$

where z is the domain with the approximate ellipse and ζ is the one with the circle. Here, ε is a measure of the eccentricity of the elliptical contour approximated, where $1+\varepsilon$ is the length of the semi-major axis and $1-\varepsilon$ is the length of the semi-minor axis. Since this is an approximate formula, the actual lengths of the semi-major and semi-minor axes, which may be found by setting $\zeta = 1$ and $\zeta = i$ respectively, are

$$a_0 = \frac{2}{1 + (1-4\varepsilon)} \qquad b_0 = \frac{2}{1 + (1+4\varepsilon)} \qquad (11)$$

Thus, we solve for the ε for which a_0/b_0 has the proper ratio (depending on the shape of the ellipse to be approximated). The mapping, eq. (10) is substituted into eq. (8) to find the complex stream function valid in the near ellipse domain. Upon differentiation of the imaginary part, one obtains expressions for the velocity in Cartesian (x,y) coordinates.

These velocities are then used, as outlined in section 1, to divide the flow domain into discrete channels over which one-dimensional (1-D) simulations accounting for phase behavior may be carried out. To determine these flow streamlines, a particle trajectory tracking method is used to integrate the velocity field. A mid-point second order explicit Runge-Kutta method is used[10]. The results given by eqs. (9) - (11) are due to Professor Milton Van Dyke of Stanford University.

If the channels are defined by the boundaries of streamlines emanating at equal angular increments around the injector, around which the flow is locally radial, each channel will have the same injection rate by symmetry (see Figure 2). Therefore, the incompressible injected fluid breakthrough time is proportional to the volume for a given channel. This provides a means for computing the individual channel volumes by using the condition that their volumes sum to the total reservoir volume. It is only necessary to insure that the volume in the longest channel (the one containing the stagnation point) is a small fraction of V (say about 1%), since the exact determination of the breakthrough time is very difficult (but not necessary) there.

Once the channels are determined, the problem has effectively been changed from a 2-D simulation into several 1-D problems. Each of these 1-D "reservoirs" has well defined shape and geometry and can be treated rigorously using a 1-D finite difference compositional model. Flow velocity, inter-phase mass transfer, and well rates can all be computed precisely. Injection is allocated into the first cell of each of these channels proportional to the angular extent about the injector subtended by their corresponding stream tubes, and production amounts are added up among them to obtain cumulative recovery and fractional flow curves (for example, Figure 3) for the entire reservoir as a function of time.

For high permeability reservoirs, the pressure gradients are small, and further simplification is possible. In this example, a linear pressure drop is used across the length of each channel from injector to producer. Such a quantity may be readily approximated by considering the pressure drop across a channel with the same length and average cross section of a stream tube. Since the permeability and the flow rate are known, the pressure drop may be obtained. This was not done to refine estimates of cross flow or residence time, but rather to approximate the effects of pressure drop on the phase split (i.e., retrograding or vaporization) of the hydrocarbon components in each streamtube.

For this example, results showed negligible sensitivity to the particular form of any reasonable pressure profile. In general, a more accurate pressure profile can be obtained by using a finite difference flow model for each channel. Alternatively, the velocity along the streamlines could be integrated back to the injector to obtain m(x,y), and this in turn used to obtain the pressure via eq. (7).

We point out that this scheme is susceptible to numerical dispersion in the same way that the usual first order upwind finite difference technique is, but the numerical dispersion is constrained to act in only one dimension. Therefore, to show that high levels of accuracy in these 1-D simulations may be attained at reasonable computing cost, it is necessary to assess the effect of streamwise numerical dispersion introduced upon discretizing each channel along the direction of flow.

The profile in Figure 4 is computed with 15 cells in the flow direction at $\theta = 0°$ (the streamtube emanating from the injector in the direction opposite to the constant pressure producing boundary). It is evident that there is a typical symmetric Fickian concentration profile indicative of numerical dispersion[11]. As the number of grid blocks increases, the semi-analytic model (SA) final recovery value approaches that obtained from a direct mass balance calculation (which simply uses the amount of injected gas to calculate the wet gas remaining and is independent of streamwise discretization), indicating the appropriate level of gridding required.

One advantage of this method is that the impact of streamwise numerical dispersion on the total effluent profile is not very severe because the majority of the channels are either far from wet gas breakthrough or they are fully swept. Only the few channels that are near breakthrough are affected. In this study, 30 cells per streamtube were used. This number appears sufficient to insure that gridding errors in gas and liquid recovery present in the SA results are well below 1% (see Table 1) and that the latter may be considered comparable to those obtained from a finite difference solution at vanishing grid size.

In contrast, the conventional finite difference models grids are not aligned with the flow directions, so that at any instant, the dispersion errors affect a large proportion of the model grids. Grid orientation effects will compound the problems further.

The wet gas recovery is given in Figure 5. Note that it is nearly 100%. This is due to the large throughput of injected gas. The final cumulative liquid recovery, shown in Figure 6, is substantially lower. The reason for this is that not all the liquid is recovered with the wet gas. First, the liquids that reside in the reservoir gas phase before the start of production can retrograde due to the declining pressure. Although some of this retrograde condensate may be stripped later by injected gas behind the displacement front, not necessarily all of it is produced. In addition, the initial saturation of residual immobile oil is made up of many different components, of widely varying molecular weight. The lighter components are readily stripped by injected gas, but the remaining resource, composed mainly of high molecular weight hydrocarbons, becomes increasingly difficult to be vaporized and recovered.

Through this model problem, we have shown that the SA is a reliable and accurate tool for simulating the gas cycling processes in which there is no rapid changes in reservoir liquid saturations. The approach is not without approximation. However, unlike in conventional finite difference models, the errors are readily estimated and bounded. It was shown that the SA can account for the complex phase behavior of the gas cycling process including retrograding and subsequent vaporization of condensed liquids, as well as pressure depletion and stripping of reservoir oil. Therefore, for 2-D problems involving gas cycling with effectively single phase, near unit mobility flow, the SA can give accurate compositional predictions which are not subject to the gridding effects normally associated with conventional reservoir simulators.

4. COMPARISON WITH FINITE DIFFERENCE MODELS

The SA can now be used to assess the effects of gridding on finite difference model (FDM) results. To check the FDM against the SA in a meaningful way, it is necessary to operate them under similar conditions. To this end, we set up a 2-D areal grid with a half-ellipse no-flow boundary. A single injector was placed in the grid block corresponding to the injector location in the SA.

Two different gridding orientations were tried in order to investigate their effect on the FDM results. The first involved a uniform 40 x 40 Cartesian grid with one of its axes aligned with the semi-minor axis of the half-ellipse. This grid imposed a constant pressure boundary condition by setting the transverse permeability of the producing boundary grid blocks much higher than the permeability of the rest of the reservoir. The second scheme involved superimposing the half-ellipse contour of the SA on a tilted 27 x 54 cylindrical polar 2-D grid with non-uniform grid block pore volumes, then setting the pore volumes of any grid blocks located outside the contour to zero. The first method was chosen for the final comparison, although we point out that liquid recoveries from the two schemes matched closely, showing reasonable independence from grid orientation effects.

Initially, the FDM was run to obtain injector-producer pressure drops for the SA. Then both models were run with the same injection and production rates. These last two sets of runs were then compared (see Figures 5-6). This procedure imposed equal throughputs (injection and production rates) on the SA and FDM in the comparison. In an average sense, the pressure histories of the models must also follow each other because of mass balance. The local pressures, however, were not identical between the two models at all times.

Through comparison against a finite difference model (FDM), the effects of gridding associated with the FDM can be estimated. In addition, differences in predictions between the two models can bring to light mechanistic effects brought about by the interaction between gridding and transport of hydrocarbon components between the liquid and vapor phases.

This comparison showed that both wet gas and liquid recoveries were lower for the FDM than they were for the more accurate SA. Recovery profiles of wet gas indicate how well the injected gas sweeps the reservoir, while those of liquid recovery also are affected by throughput of stripping gas as well as pressure. Figure 5 shows, for a test case, the behavior of the wet gas recovery with time. Figure 6 gives the comparisons between the final liquid recoveries predicted by the two models. The liquid recoveries are lower than the gas recoveries because the original reservoir liquid saturation cannot be produced as efficiently as the vapor phase components. Note also that at late times, although the SA curve had leveled off, the FDM cumulative wet gas recovery continued to rise. This was due partly to streamwise numerical dispersion causing the right side of the reservoir to remain partially unswept, with wet gas fractions as high as 80%. The region with significant amounts of wet gas remaining appeared to coincide with the shape of the unswept region as predicted by the SA at late times (see Figure 7). Here, the contours are plotted as a function of dimensionless time, which for this system is 0.125 per unit pore volume of gas injected.

Ultimate liquid recoveries predicted by the FDM were about 4% lower than those from the SA. At the level of gridding used (40 x 40), coarsening it to 20 x 20 did not greatly affect the results, which decreased only by about another 0.7%. The wet gas recovery, in all cases, was so close to 100% that the actual magnitude of the differences in recovery between the two models was small. The wet gas recoveries in the SA are actually upper bounds since they do not reflect the holdup of wet gas at the stagnation point. The reason is that after enough time, the longest stream tube in the SA will be completely swept and no wet gas will remain. In reality, however, there will always be a tiny region associated with the stagnation point which is unswept. Nonetheless, as was tested by finer discretization of the stream tubes with minimal effect, the recoveries are sufficiently accurate, since the size of this region may be made negligibly small.

It is clear that the lower wet gas recoveries predicted by the FDM are primarily due to numerical dispersion, since the displacement of wet gas by injected dry gas is strictly a plug flow process in the absence of physical dispersion. This is also evident from Figure 5, where premature injected dry gas breakthrough causes the FDM to predict lower recoveries at earlier times than the SA. At long times, however, the

additional throughput will eventually recover the remaining wet gas (left behind the front by numerical dispersion) from the reservoir, and therefore the two models' predictions will approach each other.

The liquid recoveries, on the other hand, behave differently. Figure 6 shows that the FDM liquid recoveries approximately follow the SA ones until near breakthrough. The two curves then diverge before finally approaching different ultimate recoveries at late times. Since the difference between the two models' results in this case is higher than the corresponding difference in the wet gas recoveries, and since it persists, the mechanism should be different.

These differences can be explained by a mechanism which accounts for both numerical dispersion and its resultant effect on phase behavior. The relatively coarse gridding in the FDM causes numerical dispersion which in turn allows dry gas to overrun the displacement front. This dry gas mixes with the wet gas ahead of the front causing the liquid yield (STB of liquid per MSCF of gas produced) to decrease. Moreover, the richer reservoir gas which has lagged behind the front does not have enough intermediates to stabilize the comparatively heavy liquids behind the front and therefore compensate for the effect of the leaner gas ahead of it.

In general, the ultimate cumulative oil recovery is never 100% because yield approaches zero and an economically non-vaporizable residual oil saturation is left behind. Numerical dispersion simply accelerates this process. This effect of numerical dispersion on the yield is nonlinear because the dry gas leading the front does more to decrease the yield than the wet gas lagging the front does to increase it. This is a consequence of the negative curvature of the yield versus pore volume throughput curve at early times. In other words, its negative curvature causes the average yield to always be less than the actual yield, clearly showing the indirect effect of numerical dispersion smearing out the displacement front towards decreasing final liquid recoveries.

In this comparison, it is not unusual that the FDM results did not appear to approach the SA ones. There are several factors which could explain this. The current level of gridding, even in the refined case, is still relatively coarse. In addition, the flow is inherently 2-D, and the effects of numerical dispersion are more complicated in 1-D. Shorter streamlines have more throughput and should be affected less, as would the larger ones which are not yet past breakthrough at the end of the project. Furthermore, the vaporization and retrograding of volatile oil is much more complicated mechanistically than the simple propagation of a miscible front. Thus, it would not be surprising that gridding effects would act differently under these circumstances than it would in a simple 1-D piston-like displacement.

5. CONCLUDING REMARKS

We have shown that the potential flow streamlines are applicable to compressible gas flows, and streamtube models are accurate methods for evaluating gas cycling of condensate reservoirs.

The comparison with finite difference model highlights the utility of the semi-analytical (SA) model as an alternate means of approaching a gas cycling simulation problem. Although it has many strengths, such as its absence of numerical dispersion and other gridding effects, it also has some limitations. The major one is the restriction to 2-D flow. Sometimes, due to reservoir heterogeneity, it is necessary to carry out a 3-D simulation. For this case, pending the development of a true 3-D stream tube model, it is necessary to resort to a conventional finite difference calculation. In addition, the presence of stagnation points in the flow complicates the division of the reservoir domain into channels, each having a finite residence time.

Despite these limitations, the SA model provides an efficient tool which can help increase the confidence in predictions of reservoir performance, giving recovery estimates that would otherwise require a much higher grid resolution in a conventional finite difference model. It gives an accurate accounting of flow profiles. Thus, mass transfer is confined within the stream tubes, limiting the extent of transverse dispersion. In addition, it is possible to model the complex phase behavior associated with the gas cycling process. Finally, the SA has control over its approximations. Errors can be readily approximated and then bounded. In summary, the SA represents a viable alternative to conventional reservoir simulation of the gas cycling process, as well as a benchmark against which finite difference calculations may be tested.

NOMENCLATURE

a_0	=	semi-major axis length of ellipse.
A	=	real part of source coordinate.
b_0	=	semi-minor axis length of ellipse.
B	=	imaginary part of source coordinate.
c	=	compressibility factor.
i	=	$\sqrt{-1}$
K	=	permeability.
L	=	length scale.
m	=	gas pseudo-potential.
$\mathbf{n}$	=	normal vector to boundary.
p	=	pressure.
p_0	=	reference pressure.
q	=	areal flow rate.
Q_{dry}	=	total production rate of dry gas.
Q_{wet}	=	production rate of wet gas.
t	=	time.
T	=	characteristic time for pressure transients.
V	=	reservoir volume.
x	=	x-coordinate.
y	=	y-coordinate.
z	=	complex variable.
Z	=	real gas compressibility factor.
α	=	transient decay constant, usually of order unity.

ε = eccentricity of ellipse.
ϕ = potential function.
Φ = porosity.
φ = stream function.
μ = viscosity.
θ = angle of emission from injector.
ζ = transformed complex variable.
$\langle\rangle$ = average value.

ACKNOWLEDGEMENTS

The authors thank ARCO for permission to publish this paper. They also owe the potential flow solution for a semi-ellipse domain to Professor Milton Van Dyke of Stanford University.

REFERENCES

1. Ahren, C.: "Application of Centrifugal Compressors for High Pressure Gas Cycling, Arun Field," presented at the 9th Annual Petroleum Association Convention, Jakarta, Indonesia, May 1980, 279-304.
2. Bradner, T.: "Better Technology yields more Oil," *Alaska Constr. Oil* (Dec. 1988), 20-21.
3. Ernster, G. A., Bolling, J. D., Goecke, C. R., Seader, R. A.: "A Reservoir Engineering Study of the Margham Field, Dubai, U.A.E." paper SPE 18307 presented at the 63rd Annual SPE Technical Conference, Houston, 1988, 447-462.
4. Muskat, M.: *Flow of Homogeneous Fluids through Porous Media*, McGraw-Hill, New York (1937), J. W. Edwards, Inc., Ann Arbor (1946).
5. Dake, L. P.: Fundamentals of Reservoir Engineering, Elsevier (1978).
6. Batchelor, G. K.: *An Introduction to Fluid Dynamics*, Cambridge University Press, Cambridge (1967) 189.
7. Milne-Thompson, L. M.: *Theoretical Hydrodynamics*, MacMillan and Co., London (1938) 244.
8. Kober, H.: A Dictionary of Conformational Representations, Dover (1957) 177.
9. Van Dyke, M.: Mechanical Engineering Department at Stanford University, Stanford, California. Personal communication.
10. Press, W. H., Flannery, B. P., Teukolsky, S. A., Vetterling, W. T., Numerical Recipes, Cambridge University Press, Cambridge (1986) 550-551.
11. Collins, R. E.: Flow of Fluids through Porous Materials, Reinhold, London (1961) 205.

Table 1: Channel gridding sensitivity for the SA.

Cells	Liquid Recovery	Gas Recovery
15	79.4%	97.0%
30	79.6	97.7

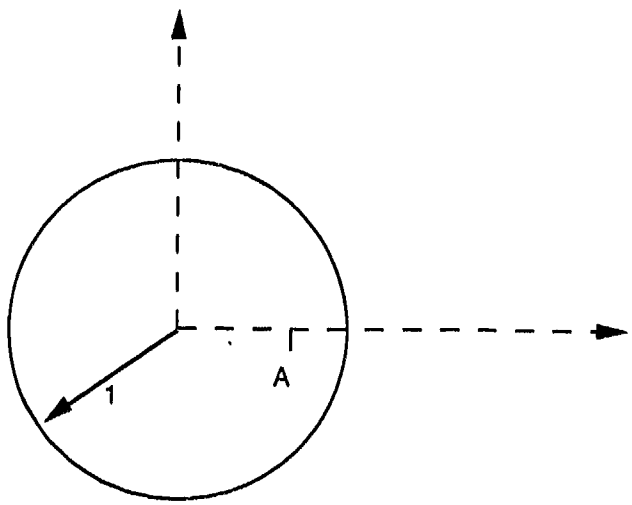

Fig. 1 -- Unit circle in the complex plane showing location of A.

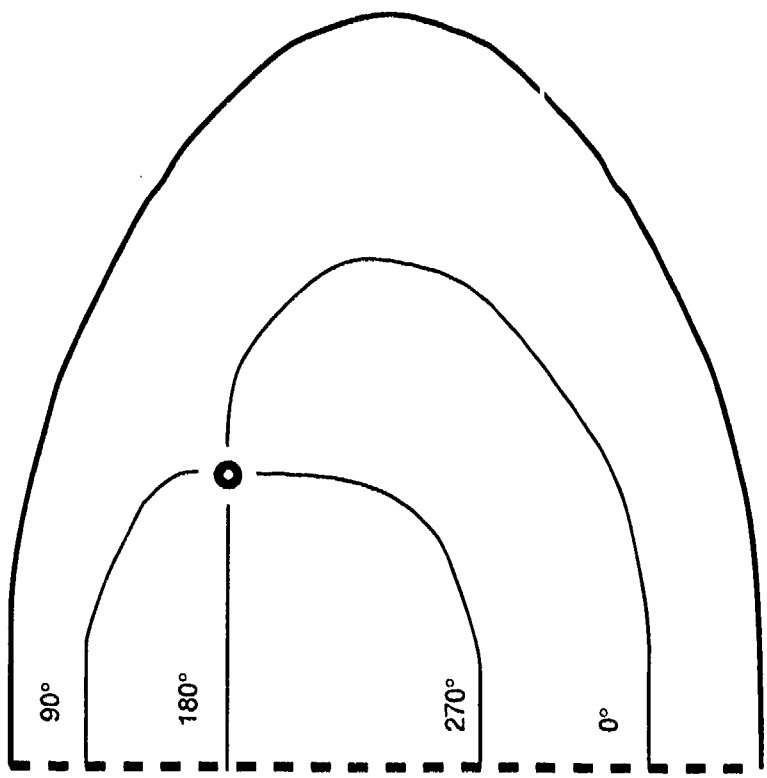

Fig. 2 -- Streamlines emanating at equally spaced angles from the injector.

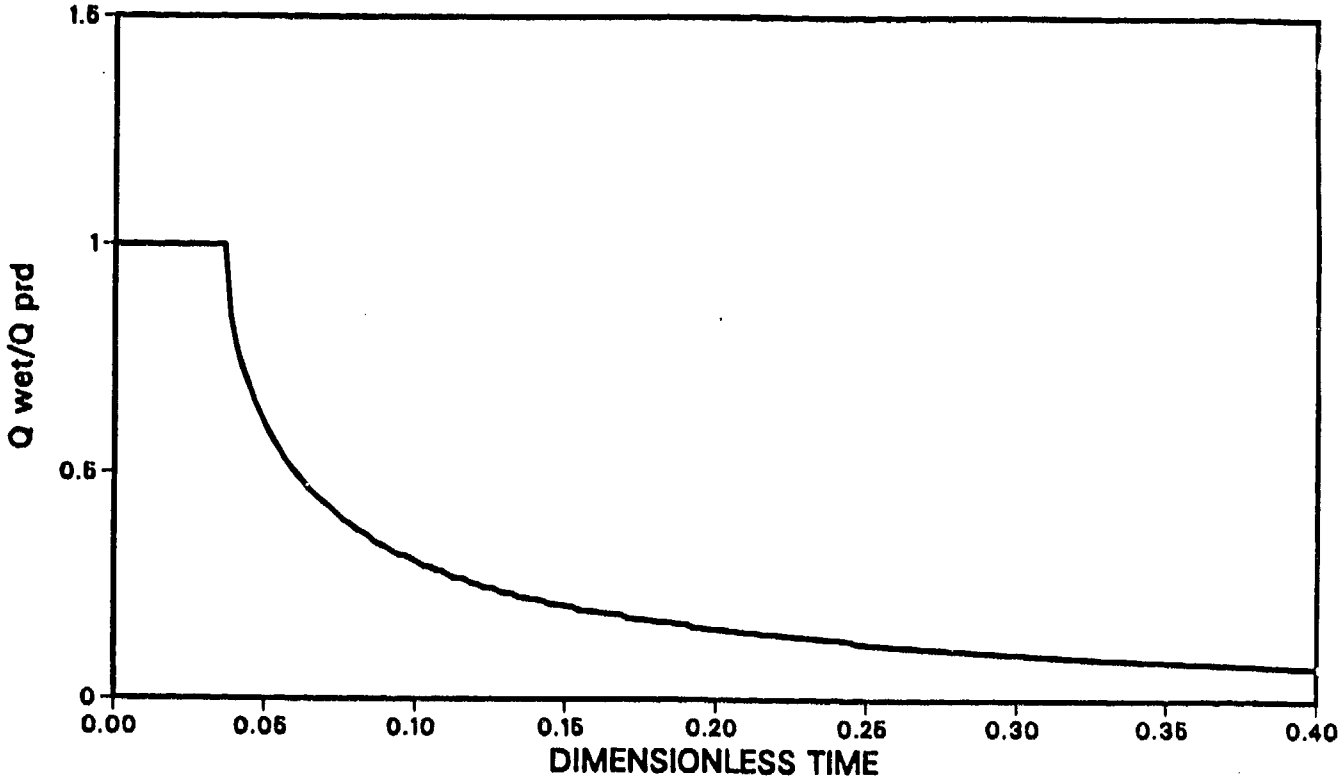

Fig. 3 -- Fractional flow of wet gas.

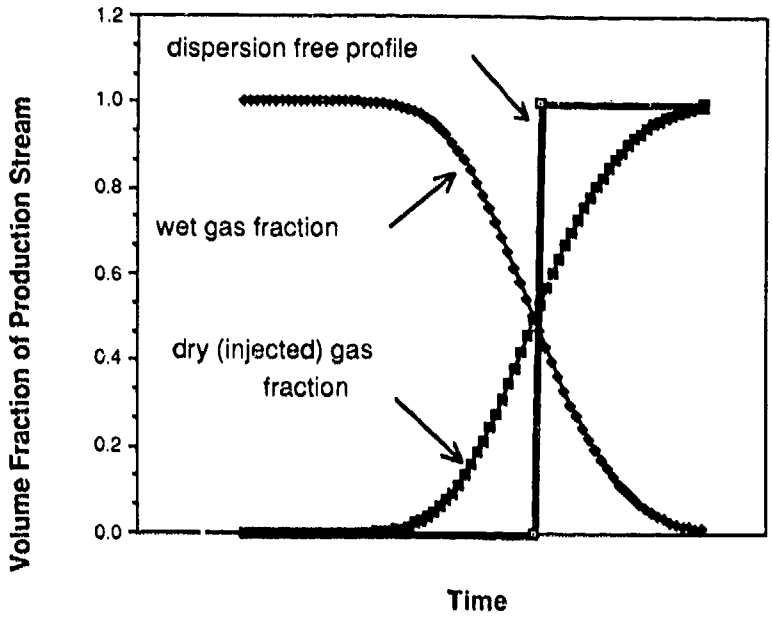

Fig. 4 -- Gas fractions from the 0° channel.

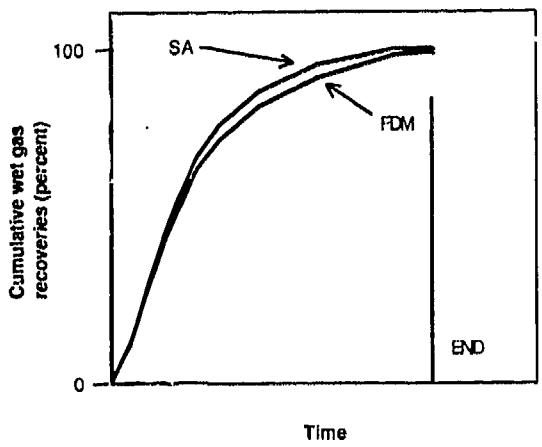

Fig. 5 -- Comparison of wet gas recovery between SA and FDM.

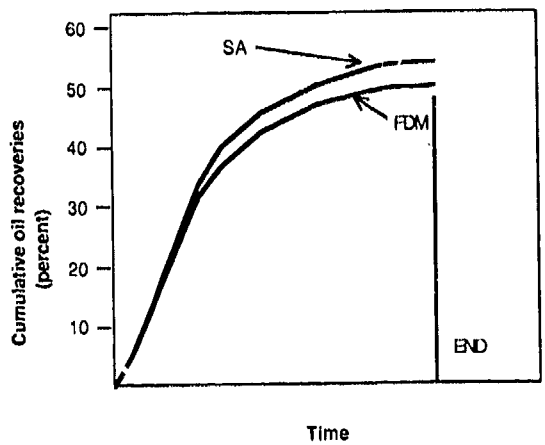

Fig. 6 -- Comparison of liquid recovery between SA and FDM.

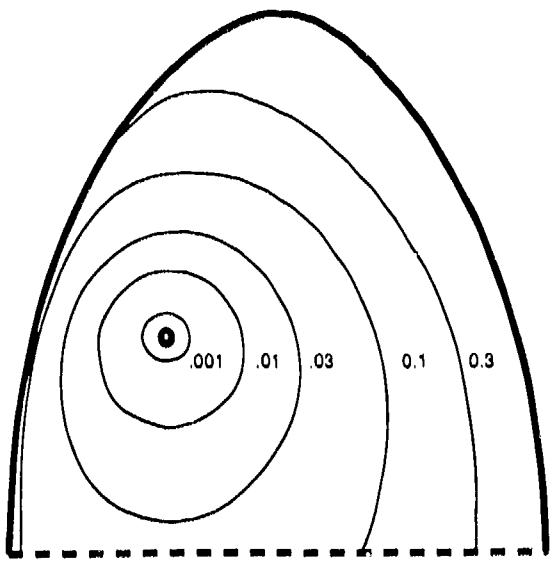

Fig. 7 -- Injected gas front at various dimensionless times.